ELSEVIER

Catalysis Today 51 (1999) 397–410

CATALYSIS TODAY

Molecular models of catalytically active sites in zeolites. Quantum chemical approach

G.M. Zhidomirov*, A.L. Yakovlev, M.A. Milov, N.A. Kachurovskaya, I.V. Yudanov

Boreskov Institute of Catalysis, Novosibirsk 630090, Russian Federation

Abstract

A brief review of quantum chemical studies of different active sites in zeolites is presented. Various factors that significantly affect the strength of Brønsted acid sites in zeolites are discussed. An interaction of zeolite protons with entrapped metal particles is considered as a reason of electron-deficiency of metal clusters in zeolite cavities on the Pd and Pt species as an example. Probable precursors of Lewis acid sites (LAS) and reliable molecular models of the LAS in zeolites are discussed on the basis of quantum chemical analysis. Transition metal ions can be catalytically active in the lattice or extra-lattice zeolite positions and the two possibilities are considered for selective oxidation site in titanium silicalite and FeZSM-5 zeolite catalysts, respectively.

Keywords: Acid sites; Zeolites; Epoxidation

1. Introduction

Nowadays, it is widely recognized that intermediate chemical interaction of the reactants with certain groups of atoms of a catalyst plays a key role in the mechanism of chemical catalysis. Such groups of atoms are usually referred to as active sites (AS). Detection of AS, study of their formation, structure and chemical properties become, at present, one of the main objectives for fundamental research in catalysis.

Zeolites are known to be very efficient catalysts in a number of chemical processes. Their catalytic activity is associated with different AS such as:

1. Brønsted acid sites;
2. Lewis acid sites;
3. metal ions in cationic positions;
4. transition metal ions in zeolite lattice positions;
5. extra-lattice transition metal compounds in channels and cavities of a zeolite;
6. metal particles in zeolite cavities.

Molecular modeling of the active sites mentioned above and quantum chemical calculations of their geometric structure and electronic state may be very useful for a better understanding of their chemical properties [1]. Another goal of quantum chemical consideration is the structural interpretation of spectroscopic investigation of an AS in zeolites. Infra-red spectroscopy study with use of probe molecules (CO, NO, $NCCH_3$, etc.) is a powerful method for identification and structural investigation of active sites. In the following, considerable attention will be paid to quantum chemical treatment of such experimental data.

As a rule, an AS is a local structure on the catalyst surface. Therefore, it is reasonable to use the so called

*Corresponding author.

0920-5861/99/$ – see front matter
PII: S0920-5861(99)00029-2

molecular cluster approach in quantum chemical calculations. According to it, some finite fragment is cut off the lattice. The fragment choice is determined by features of the process under study. The cluster approximation is rough since it is necessary to break the bonds between the cluster and the rest of the lattice. There are various ways to decrease the negative effect of the bond breaking. The saturation of dangling cluster bonds with some boundary monovalent atoms, for example with hydrogen, or atoms with specially fitted quantum chemical parameters (''pseudoatoms'') is one of the simplest and most suitable ways to describe better the features of the system under study [2].

2. Brønsted acid sites (BAS)

Bridged hydroxyl group of a zeolite is a typical example of a BAS on the surface of a heterogeneous catalyst. The $(HO)_3SiOHAl(OH)_3$ cluster is the simplest model of a bridged hydroxyl group [2,3]. The deprotonation energy of the bridged hydroxyl was shown by semiempirical and ab initio calculations to be less than that of a terminal hydroxyl in silica and alumina [3]. Acidic properties exhibited by such structures may be considered as resulting from the OH group coordination by the neighboring electrophilic atom. One can say that the high acid strength of the bridged group ≡Si–OH–Al≡ compared to that of the terminal ≡Si–OH is due to the solvation of the $\equiv Si–O^-$ anion by the Lewis acid Al≡ [1,4,5]. There is remarkable experimental correlation (Fig. 1) between the proton-donor ability of a BAS of the type T_1-OH···T_2 and the coordination strength of a LAS T_2 for the series of heterogeneous zeolite catalysts (T_1=Si; T_2=B, Be, Fe, Ga, Al) [6]. Here, the PA^C quantity is the proton affinity of the acid residue of the BAS of the catalyst and Q_{CO} is the coordination energy of a CO molecule to the T_2 Lewis acid. One can see that energy of the proton abstraction from the OH group, $E(H^+)=PA^C$, decreases with an increase of Q_{CO}. The quantity PA^C can be characterized by a shift in the OH stretching frequency, $\Delta\omega_{OH}$, upon adsorption of a molecule of a base B (e.g. CO) via formation of a hydrogen bond such as B···H–O(T_1)T_2. Similarly, the quantity Q_{CO} can be found from the shift of the CO stretching frequency upon adsorption at a Lewis acid site.

Zeolites often contain BASs of different acidic strength and various IR spectroscopic characteristics of the bridged OH group. Quantum chemical treatment of a chosen series of cluster models of different BASs have been rather successful in understanding their complicated nature [3,7,8]. Considering the influence of local factors, which are as a rule most important it is reasonable to discuss separately the ''chemical'' and ''structural'' factors as shown in Fig. 2 [8]. Calculations were carried out on the STO-3G level. The ''chemical'' factor means the substitution of a Si atom by Al and H on the periphery of the cluster. Structural deformations responsible for different geometries of the fragments in the lattice were modeled by displacement of the terminal H atoms in the $H_3Si–OH–AlH_3$ cluster from their equilibrium positions. These atoms were frozen in their non-equilibrium positions while the rest of the molecule was optimized. The principle conclusion was

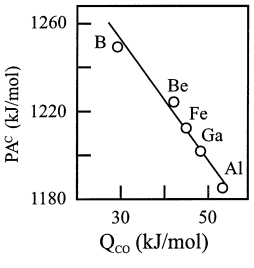

Fig. 1. Experimental correlation between the proton-donor ability of BAS of the type T_1-O···T_2 and the coordination strength of the T_2 as a LAS for isomorphically substituted zeolites.

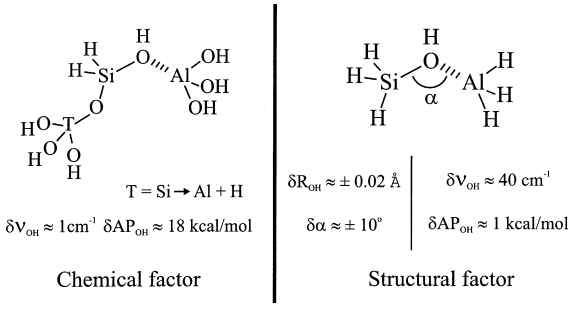

Fig. 2. Cluster structures which are used for the comparative ab initio calculations of the role of ''chemical'' and ''structural'' factors.

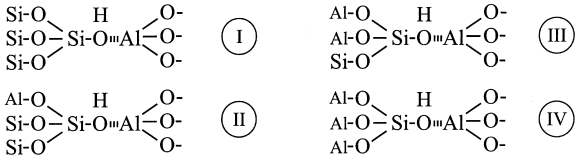

Fig. 3. Molecular structures of the four main bridged hydroxyl species according to the decrease of acid power from I to IV.

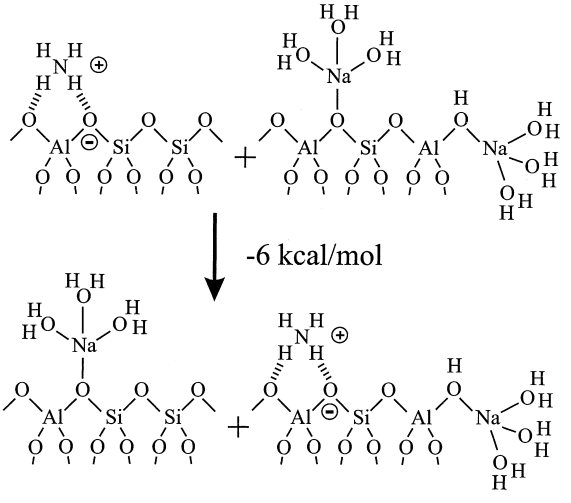

Fig. 4. Cluster models used in the calculation of the preferability of different zeolite lattice sites for the $Na^+ \rightarrow NH_4^+$ substitution reaction.

made that ''chemical'' factor is mainly responsible for changes in acidic strength of a BAS in zeolites. On this ground, a classification of BAS acidic strength was proposed [7] (Fig. 3). The structural factor is the most important one for the changes in ω_{OH} of the bridged OH groups.

Usually an H-form of a zeolite is obtained via ammonium exchange. Calculations indicate (Fig. 4) that M^+ substitution for NH_4^+ is energetically preferable at sites with a higher concentration of Al atoms and show that the initial exchange stage yields the weakest BAS [9] in agreement with the experiment.

3. Electron-deficient state of metal particles in zeolites

The change of electronic structure of a metal particle (MP) encapsulated in a zeolite cavity is a part of a general problem of metal-support interaction in supported catalytic systems. The zeolite lattice can act like an electron-acceptor or electron-donor with respect to the MP. This results in electron-deficient or electron-enriched states of the particle, respectively [10,11]. An electron-deficient state of the metal particle can be observed by blue shift of the CO stretching frequency (ω_{CO}) by a red shift of the M–C stretching frequency (ω_{MC}) or by a decrease of the adsorption energy of a CO molecule. This state of the MP is interesting from the point of view of catalytic application. For example, positively charged metal species exhibit higher catalytic activity in hydrogenation and hydrogenolysis as well as higher resistance to sulfur poisoning.

FTIR spectroscopy of adsorbed CO has been used to study the state and dispersion of platinum in mordenite [12]. The IR adsorption band at 2123 cm^{-1} was assigned to isolated Pt atoms anchored by zeolite protons. This supposition is based on the following observations: (i) the position of the band does not depend on the CO coverage; and (ii) the presence of the band depends on the presence of zeolite protons. If the latter are neutralized or replaced by Na^+, the band at 2123 cm^{-1} disappears. The unusual magnitude of the shift of -20 cm^{-1} (ω(CO)free=2143 cm^{-1}) was rationalized as a consequence of electron-deficiency of the Pt atom. The platinum atoms are considered to reside in side-pockets of the main channels of the mordenite [12].

The hypothesis that the observed platinum form can be assigned to a Pt atom anchored by protons of the zeolite hydroxyl groups was justified by density functional calculations of model clusters [13].

Cluster models of Zeolite–Pt–CO species (Z–Pt–CO (a) and Z_2–Pt–CO (b)) are presented in Fig. 5. Here, the H_3Si–OH–AlH_3 moiety is denoted as Z. Besides that, simplified cluster models $(HOH)_n$–PtCO (n=1–3) and ClH–PtCO were calculated in order to elucidate the dependence of observables on the strength and number of the acidic hydrogen atoms bonded to Pt. An alternative model of the Pt–H interaction, H^+–PtCO, was calculated in contrast to the anchored PtCO moiety. This type of interaction exemplifies an extreme case of Brønsted acid–metal interaction. The models were calculated employing the scalar-relativistic first-principles linear combinations of Gaussian-type orbitals density functional (LCGTO-

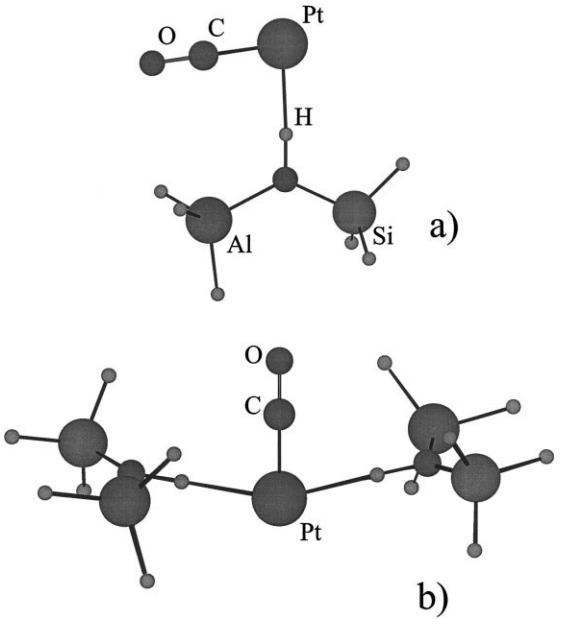

Fig. 5. Calculated structures of cluster models of Pt, anchored by (a) one and (b) two protons of a BAS in HMor and interacting with a probe CO molecule.

DF) method [14]. The exchange-correlation density functional was applied in the local density approximation.

The results of calculations are presented in Table 1. The Pt 4f core level energy shift may serve as an approximate measure of the charge state of the Pt center in the complexes. Going from the complex of a Pt atom with one H_2O molecule to that with HCl and then to the structure Z–Pt–CO, one notes a rather close correlation between the frequency shifts $\Delta\omega$(CO) and the core level shifts $\Delta\epsilon$(Pt 4f). A negative value of the core level shift implies an increasing positive charge on the Pt atom in the series mentioned. One can expect that the Brønsted acidity of the hydrogen atoms increases in the series $H_2O \rightarrow HCl \rightarrow Z$. Indeed, the red shift $\Delta\omega$(CO) of the CO vibrational frequency in the series was found to decrease (in absolute value), $-76 \rightarrow -60 \rightarrow -43\ cm^{-1}$. The model complexes in which the Pt atom is anchored by one or two zeolitic OH groups yield C–O vibrational frequency shifts of -43 and $-40\ cm^{-1}$, respectively, in reasonable agreement with the experimental value of $-20\ cm^{-1}$. Thus, one may conclude that these complexes represent adequate models of electron-deficient atomic platinum species in Pt/HMor. The value of the C–O vibrational frequency shift calculated for the complex H^+–Pt–CO is positive, $+37\ cm^{-1}$ (Table 1), at variance with the experimental value of $-20\ cm^{-1}$. Therefore, in light of the results of both our density functional calculations and experiment [12], a direct protonation of Pt–CO species in mordenite seems to be unlikely.

Palladium particles of 5–7 Å diameter have been detected in faujasites. Sachtler et al. [15] have suggested that these particles are of nuclearity 13 and that they are able to interact with zeolite protons. The electron-deficient state of the small Pd clusters in Pd/NaHY has been deduced from the observation of unusual vibration frequency of adsorbed CO,

Table 1
Calculated characteristics for the Pt–CO moiety bound to different substrates

System	R(Pt–H) (Å)	$\Delta\epsilon$(Pt 4f) (eV)	$\Delta\omega$(CO) (cm^{-1})	E_b (eV)
Pt–CO	–	–	−73	–
H^+–Pt–CO	1.54	−8.73	+37	–
Z–Pt	1.85	–	–	0.93
HOH–Pt–CO	1.97	−0.41	−76	0.26
$(HOH)_2$–Pt–CO	1.97	−0.73	−63	0.46
$(HOH)_3$–Pt–CO	2.06	−1.12	−47	0.80
ClH–Pt–CO	1.94	−0.74	−60	0.44
Z–Pt–CO	2.00	−1.13	−43	0.62
Z_2–Pt–CO	2.01	−1.97	−40	1.08
Z(4r)–Pt–CO	2.20	−0.38	−84	1.69

Pt–H interatomic distance, R(Pt–H); Pt 4f electron binding energy shift with respect to that in Pt–CO, $\Delta\epsilon$(Pt 4f); CO frequency shift relative to free CO, $\Delta\omega$(CO); and H–PtCO binding energy, E_b.

1860 cm^{-1}. This frequency was interpreted as blue-shifted infrared band from 1823 cm^{-1}. The latter corresponds to a stretching of CO molecule triply bonded either to a small neutral palladium species in zeolites [15] or CO adsorbed on the Pd(1 1 1) surface.

Density functional calculations of free and protonated tetrahedral and octahedral clusters Pd_4 and Pd_6 have been carried out [16] employing a gradient-corrected energy functional. These clusters were chosen as the simplest models of tetrahedral and octahedral interstitial positions of the bulk Pd. The models were designed to aid in understanding at the molecular level the protonation of palladium clusters in zeolites as well as the proton-induced changes in the adsorption properties of the clusters with respect to CO molecules.

The LCGTO-DF code [14] with non-local exchange-correlation density functional was employed for calculation of the models. The cluster geometries were optimized under the following symmetry constrains: T_d for Pd_4 and $[Pd_4H]^+$, C_{3v} for Pd_4CO and $[Pd_4H]^+$–CO, O_h for Pd_6, $[Pd_6H]^+$ and for the metallic core of these clusters with adsorbed CO. Calculated atomization energies, 4.19 eV for Pd_4 and 7.84 for Pd_6, indicate high stability of the clusters. The protonation of the palladium clusters elongates the Pd–Pd distance (ΔR=0.18 Å for Pd_4, but only 0.05 for Pd_6). The calculated protonation energy of the palladium clusters under consideration provide a crucial check for the hypothesis on the formation of protonated $[Pd_nH_x]^{x+}$ species in Pd/NaHY catalyst. The calculated values, 9.4 and 9.9 eV for Pd_4 and Pd_6, respectively, even exceed the proton affinity of an ammonia molecule (8.8 eV). The NH_3 molecule is known to form NH_4^+ as a result of protonation in the H-form of zeolites. Thus the present data support the assumption that electron-deficient metal species can be formed by the protonation of Pd clusters entrapped in zeolites. The calculation results are presented in Table 2. The Pd_n–CO binding energy decreases by 0.39 and 0.33 eV upon protonation of the Pd_4 and Pd_6 substrate species, respectively. Calculated blue shifts ($\Delta\omega_{CO}$) of triply bonded CO as a result of protonation of the clusters are 99 cm^{-1} for Pd_4 and 82 cm^{-1} for Pd_6. Although the calculated shifts are in the proper direction, they are too large when compared to experimental data (37 cm^{-1}). A better agreement of theory with experiment will probably be achieved by means of increasing the cluster size (for example, up to Pd_{13}).

The effect of cluster protonation on its adsorption properties with respect to molecular hydrogen was studied by means of the density functional approach. The following cluster models were calculated: Pd_4, Pd_4H_4, Pd_4H^+, and $Pd_4H_5^+$. Some of them are presented in Fig. 6. The main result is that the protonation of the neutral clusters slightly increases the adsorption energy of the first H_2 molecule, 1.46 and 1.73 eV for adsorption on Pd_4 and Pd_4H^+, respectively, but at the same time significantly decreases that of the second one, −0.72 and −2.74 eV for adsorption on Pd_4H_2 and $Pd_4H_3^+$, respectively. From these results, it follows that a H/Pd ratio equal to 0.5 may be easily achieved upon H_2 adsorption for both electron-deficient (protonated) and neutral palladium clusters. Taking into account possible deficiencies of the models, one can conclude that a ratio close to unity might be reached for neutral clusters but not for charged ones in line with experiment [17].

Table 2
Calculated and experimental results for palladium substrate clusters with a μ_3-adsorbed CO molecule: interatomic distances, R, CO adsorption energies, E_{ads}, and shifts of the CO stretching frequency with respect to free CO, $\Delta\omega_e$ [a]

Model	R(Pd–Pd) (Å)	R(Pd–H) (Å)	E_{ads} (eV)	$\Delta\omega_e$ (cm^{-1})
Pd_4–CO	2.83, 2.75	–	2.35	−418
Pd_6–CO	2.73	–	1.58	−415
Pd_n–CO exp	–	–	1.30	−320
$[Pd_4H]^+$–CO	2.82, 3.10	1.93, 1.60	2.22	−304
$[Pd_6H]^+$–CO	2.78	1.97	1.25	−333
$[Pd_nH]^+$–CO exp	–	–	–	−283

[a] Reference values for the vibrational frequency of free CO: calculated ω_e(CO)=2163 cm^{-1}, experimental ω(CO)=2143 cm^{-1}.

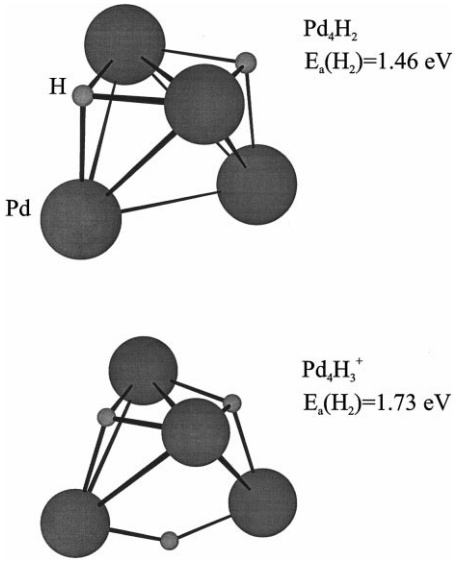

Fig. 6. Cluster models for the calculation of H_2 adsorption on palladium and protonated palladium clusters.

4. Lewis acid sites

LAS appear in heterogeneous catalysts due to thermo-vacuum treatment. The resulting structures of LAS depend on the properties of the lattice (rigid or flexible) and on the treatment conditions. Thus, a theoretical study of LAS should take into account the process of LAS formation in order to find a realistic molecular structure of LAS for the system under study. On the other hand, such calculations require information on LAS precursors (parent chemical species of LAS). Generally speaking, there are two variants: (i) these species belong to the zeolite framework (there are interesting speculations on such a possibility but up to now no reliable experimental evidence exists); (ii) non-framework species that can be formed during dealumination of zeolite (experimental investigations show that such species can be LAS precursors). The modeling of zeolite dealumination was performed in [9], in which possible ways of transformation of four-membered rings with two Al ions were analyzed, see Fig. 7. Subsequent condensation of such types of initial hydroxide structures will give rise to boehmite-like structures [18]. As a common result, the close similarity between the LAS formed from extra-lattice aluminum oxide–hydroxide species and the LAS on the surface of transition alumina can be expected, in qualitative agreement with experimental data.

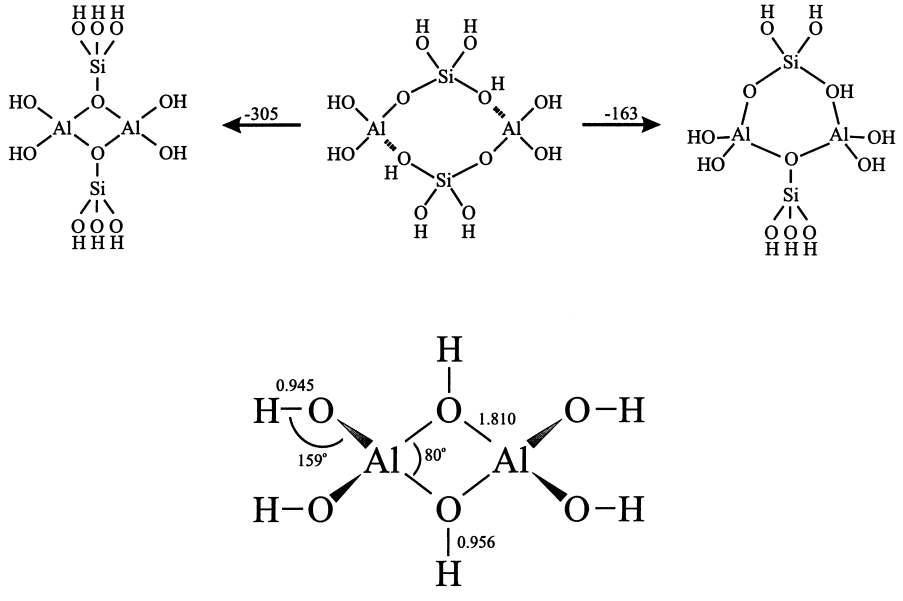

Fig. 7. Possible versions of the reconstruction of a model four-membered zeolite ring in the H form of zeolites. The calculations have been carried out with a STO-3G basis set. The geometry of the $(OH)_2Al{=}OH_2{=}Al(OH_2)$ molecule have been calculated with the 3-21G basis set (D_{2h} point symmetry).

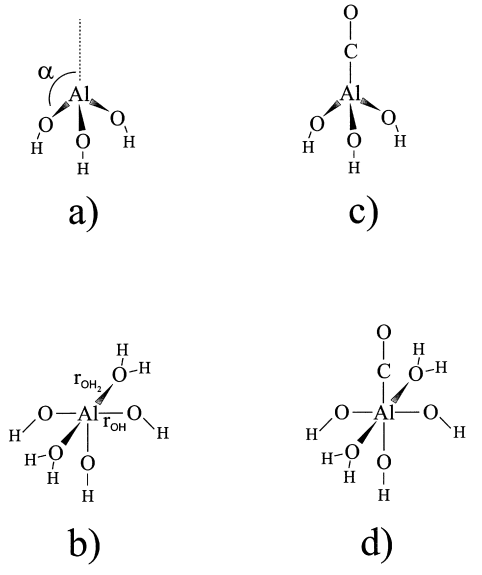

Fig. 8. A cluster model of a LAS with (a) 3- and (b) 5-coordinated Al^{3+} and (c,d) their adsorption complexes with a probe CO molecule.

Based on the spinel structure of γ-Al_2O_3, two types of LAS, three- and 5-coordinated Al ions, Al^{3+}_{3c} and Al^{3+}_{5c} are usually proposed in this system. The precursors of these are, respectively, Al ions in tetrahedral and octahedral positions of the crystal structure.

Conventional cluster models for these sites [19–21] are shown in Fig. 8. These cluster models are minimal but their use is reasonable. The high-level calculations of adsorption complexes become possible, and in many cases, for example, in the case of CO coordination by LAS, this point is very important. This approach then allows one to avoid the arbitrariness in the choice of clusters.

Unfortunately, these minimal cluster models are also not free from intrinsic uncertainties. As for $Al(OH)_3$, there is the problem of the position of the Al cation relative to the plane of three surrounding oxygen anions, i.e. the height of the AlO_3 pyramid. A model $Al(OH)_3(OH_2)_2$ of the LAS with 5-coordinated Al^{3+} can be considered in two variants: one with equal Al–OH and Al–OH_2 distances or others with different distances according to the optimization procedure.

The possible influence of these uncertainties in the geometrical structures of discussed cluster models has been considered in [22] for the example of adsorption of the CO molecule. Three structures of Al^{3+}_{3c} with different angle α, have been considered as shown in Fig. 8. In addition, two structures, according to the variants mentioned above, have been discussed for Al^{3+}_{5c}. These calculations have been performed using the LCGTO-DF method [14] with the parametrization of exchange-correlation interactions suggested by Vosko, Wilk and Nusair (VWN). After achieving self-consistency, gradient corrections to the exchange and correlation energy functionals (BLYP) were computed using VWN electron density in order to improve the description of the clusters energetics.

Table 3
Structural and vibrational data, calculated at the BLYP level for CO, adsorbed on 3- and 5-coordinated Al^{3+} LAS for different methods of cluster model construction

Model	α	r_{OH} (Å)	r_{OH2} (Å)	$\Delta\omega$(CO) (cm^{-1})
Al^{3+} 3-coord.	109.5	1.74	–	85
Al^{3+} 3-coord.	100.0	1.74	–	84
Al^{3+} 3-coord.	90.0	1.74	–	63
Al^{3+} 5-coord.	90.0	1.86	1.86	30
Al^{3+} 5-coord.	90.0	1.79	2.04	28

The results of these calculations are represented in Table 3. It is necessary to note the closeness of the results for the most reliable models of Al^{3+}_{3c} with α=109.5° and 100° and for both models of Al^{3+}_{5c}. The effort to assign the results of calculations of ω_{CO} shift upon CO adsorption has resulted in the probable assignment of the experimental data represented in Table 4. The assignment proposed in [23], is also represented there. The most interesting conclusion is about formation of a 4-coordinated LAS, Al^{3+}_{4c}.

This is why the construction of a cluster model for 4-coordinated LAS Al^{3+}_{4c} according to the models considered above should be a logical development of this work. At the same time, it would be interesting

Table 4
Assignment of experimental data on IR shifts of CO adsorbed on LAS of γ-Al_2O_3

$\Delta\omega$CO (exp.) (cm^{-1})	Zecchina et al. [23]	Calculated [22]
A (70–90)	Defects	3-Coord. Al^{3+}
B (50–70)	3-coord. Al^{3+}	4-Coord. Al^{3+} assumed
C (20–40)	5-coord. Al^{3+}	5-Coord. Al^{3+v}

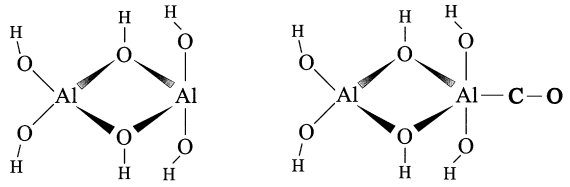

Fig. 9. A cluster model of a LAS with 4-coordinated Al^{3+} and its adsorption complex with a probe CO molecule.

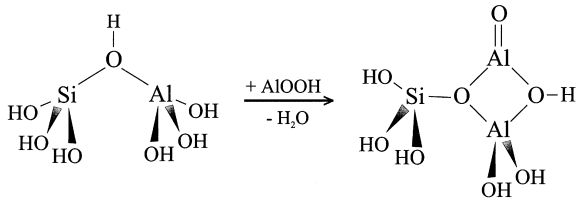

Fig. 10. A possible variant for the formation of an "unusual" type LAS in a zeolite; the calculated energy of this process $\Delta E = -205.4$ kJ/mol.

to check the stability of the structural conclusions to a possible variation of the computational scheme, in particular, to the use of other basis sets and exchange-correlation potentials. It should be noted that the construction of the molecular model of 4-coordinated LAS in full analogy with the 3- and 5-coordinated LAS (see Fig. 8) would give rise to a non-symmetrical structure of the cluster, which seems to be unjustified. This is why the binuclear cluster was chosen as a minimal one as represented in Fig. 9 [24].

The calculations of these cluster models of 3-, 4- and 5-coordinated LAS were performed [24] using the DFT method (Gaussian 92/DFT package), standard basis set 6-31G*, exchange functional Becke88 and correlation functional Perdew86. For the Al^{3+}_{3c} cluster model, we assumed α=100°; for the Al^{3+}_{5c} model, we assumed all Al–O distances to be equal; and for the Al^{3+}_{4c} model, we assumed the AlOOAl fragment to be planar. The results of these calculations (the ω_{CO} frequency shifts and estimated CO adsorption energies) are represented in Table 5.

Two interesting features can be seen there. The first is the close similarity of the CO frequency shifts for Al^{3+}_{3c} and Al^{3+}_{5c} to those reported in [22]. This means that the assignment of experimental data, proposed in [22] for these types of LAS is stable to changes in the scheme of calculations. The second feature is that the calculated value of the CO frequency shift for Al^{3+}_{4c} lies between those for Al^{3+}_{3c} and Al^{3+}_{5c}. Therefore, this is one more important argument for the hypothesis concerning the assignment of band B in the IR spectra to the Al^{3+}_{4C} LAS as proposed in [22]. It is interesting that the supposition of the existence of a 4-coordinated LAS is also confirmed by the molecular dynamics simulations [25], where the authors reported the relative amounts of the different types of LAS on the surface of γ-Al_2O_3; these were 221, 1229 and 874 for LAS with 3-, 4- and 5-coordinated Al^{3+}, respectively. It can be seen that there must be a relative predominance of the 4-coordinated LAS on the surface.

Table 5
Structural and vibrational data calculated at the BP86 level for CO adsorbed on 3-, 4- and 5-coordinated Al^{3+} LAS

Coord. of Al^{3+}	$\Delta\omega$(CO) (cm^{-1})		E_{ads}(CO) (kJ/mol)	
III	84	82	83.9	100.5
IV	–	48	–	84.9
V	30	27	32.8	50.1

The results from [22,24], respectively, are presented in the left and right columns for each variable.

There exists the question of the possibility of LAS formation in zeolites not connected with the preliminary formation of extra-lattice aluminum hydroxide–oxide species. As mentioned above, one of such ways could be connected with the earlier stages of the dealumination process and with the migration of active species such as AlO^+ and AlOOH, in the lattice. A possible mechanism of such type LAS formation is represented in Fig. 10. The energetics of such process was estimated using the calculation scheme mentioned above.

A LAS of this type was discussed previously in [26]. It contained a gallium atom and was considered as a

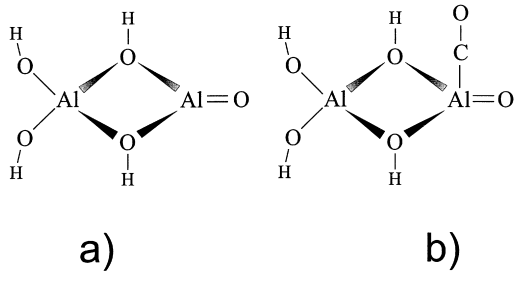

Fig. 11. A cluster model of an "unusual" LAS (a) used in calculations of the adsorption of a probe CO molecule (b).

model of the active site in the process of methane activation. Using the above calculation technique, we have computed the frequency shift of CO adsorbed on such a LAS (Fig. 11), and have estimated the energetics of this process [24]; $\Delta w(\mathrm{CO}) = -31.6\ \mathrm{cm}^{-1}$, $E_{ads}(\mathrm{CO}) = 46.2$ kJ/mol. The most remarkable result of these calculations is that the CO frequency substantially decreases upon adsorption on such a LAS, this being opposite to the shift observed in complexes of CO with 3- and 5-coordinated LAS.

Now there is no direct experimental data that LAS of this type really exist and this may stimulate further experimental investigations.

5. Hydrocarbon selective oxidation sites formed upon decomposition of N_2O in FeZSM-5 zeolites

FeZSM-5 zeolites exhibit extremely high catalytic activity in the selective oxidation of various compounds (alkanes, benzene, carbon monoxide) by dinitrogen monoxide [27]. These processes involve adsorption and decomposition of N_2O:

$$N_2O + Z \rightarrow N_2O \ldots Z \quad (1)$$

$$N_2O \ldots Z \rightarrow N_2 + OZ \quad (2)$$

where Z and OZ in this case denote an active site in FeZSM-5 and the oxidizing center, respectively. In particular methane is converted to methanol with an almost 100% yield

$$CH_4 + OZ \rightarrow CH_3OH \ldots Z \quad (3)$$

The knowledge of the Z and OZ structure is the key for understanding their activity. The first molecular model of the Z center was suggested [28] to have the form of the lowest-spin binuclear cluster. Its structure was considered to be the result of the partial dehydration of an extra-framework Fe(III) hydroxide dimer. The formation of such an extra-framework compound was suggested by analogy with the formation of extra-framework Al(III)-hydroxide dimers during the dealumination of zeolites [8].

Quantum chemical calculations of stages (1)–(3) were performed at the MP2/HF/LANL1DZ level with the above-mentioned binuclear cluster as the Z moiety [29]. The resultant structures are shown in Fig. 12. The calculations predict the possibility of the formation of the bridged peroxide structure (Fig. 12(b)) which can decompose methane with an insignificant activation energy.

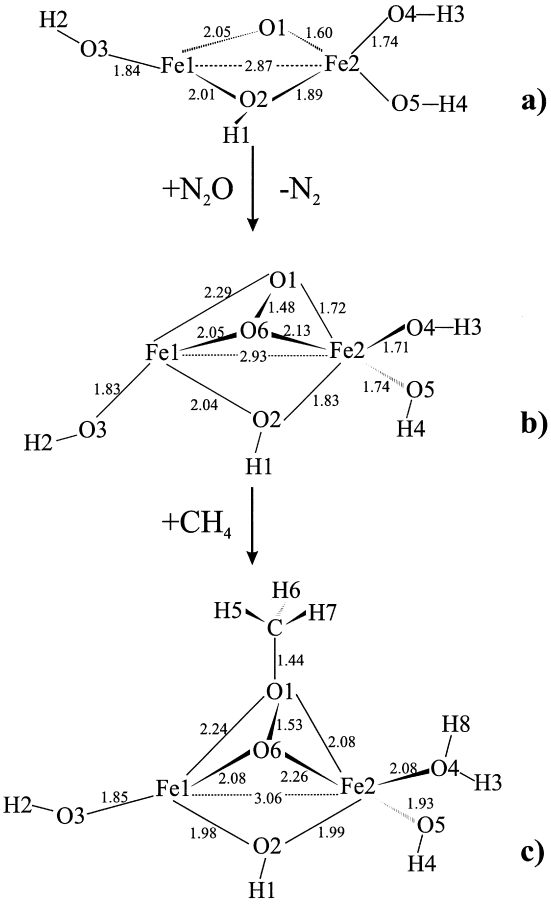

Fig. 12. Cluster models for the conversion of a binuclear Fe hydroxide structure: (a) after partial dehydroxylation, (b) after decomposition of N_2O, (c) after dissociative addition of CH_4. (MP2/HF/LANL1DZ calculations).

The model of free hydroxide binuclear cluster, is of course, a very rough approximation, because interaction with zeolite framework should apparently be taken into account. Possible ways of forming the extra-lattice Fe-oxide species bound to zeolite framework are shown in Fig. 13. A cluster model of structure presented in Fig. 13(a) and its transformations due to interaction with the N_2O and CH_4 molecules are shown in Fig. 14. The calculations were carried out employing the semiempirical NDDO/MC method [30]. As in previous studies, the possibility of the

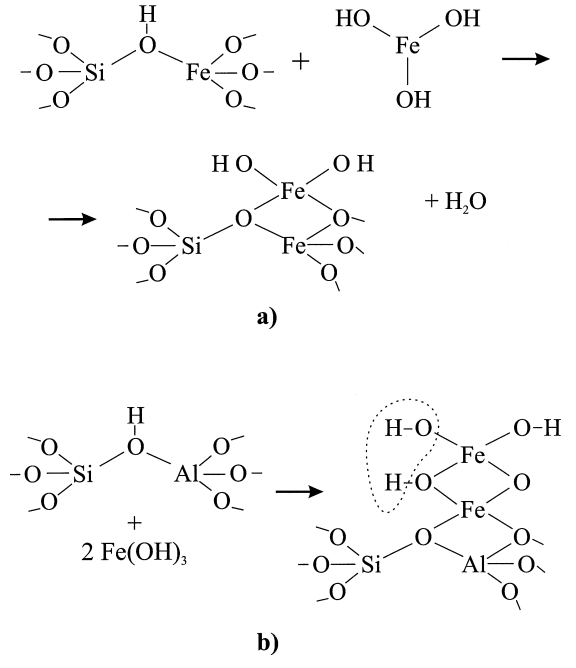

Fig. 13. Schemes for the probable formation of extra-lattice Fe-oxide species in zeolites: (a) in FeZSM-5, and (b) in AlZSM-5.

formation of both ferryl and bridged peroxide structures as a result of N_2O decomposition should be noted. The calculations also show that the complexes are rather reactive towards CH_4. More reliable estimations of the energetics of the processes require high level ab initio calculations.

6. Selective hydrocarbon oxidation sites in titanium silicalites

In recent years, a lot of attention has been focused on titanium-containing zeolites because of their remarkable catalytic properties in the oxidation of hydrocarbons by H_2O_2 solutions. A number of investigations have been carried out to elucidate the structure of microporous Ti-silicalites (TS-1, TS-2) containing a small percentage of Ti substituting for Si (1–2%). Although the local structure of the titanium site in silicalite is still under discussion, the model of isomorphous substitution for Si in tetrahedral framework positions is the most consistent with experimental data. However, it is not clear how a tetrahedral framework titanium species can show catalytic properties.

It has been hypothesized that one or two Si–O–Ti bridges can be hydrolyzed without destroying the fourfold coordination [31–33]. Addition of H_2O_2 gives rise to a strong UV–Vis peak at 26 000 cm^{-1}. This band is associated with charge transfer from a peroxo-type species to the Ti atom [31]. This process is accompanied by consumption of hydroxyl groups and hence by a change in the 48 000–50 000 cm^{-1} band. However detailed information on the local structure of the active species is still lacking. Different authors have suggested that the formation of titanium-peroxo- or hydroperoxo-complexes occurs as a result of the interaction of a framework titanium site with H_2O_2. However, most of the well-characterized titanium peroxo-complexes $Ti(O_2)$ are not active in oxidation reactions, in particular in the epoxidation of alkenes, the hydroperoxo–titanium group Ti–OOH is therefore thought to be responsible for the epoxidation of alkenes [34]. Although no hydroperoxo–titanium compounds have yet been isolated, it has been argued that Ti–OOR species (R=Alkyl, Aryl) are the oxidants in the epoxidation of alkenes with alkyl or aryl hydroperoxides catalyzed by silica-supported titanium oxide catalysts [35]. Evidence has been presented to show that the tetraphenylporphyrin titanium peroxo-complex, $(TPP)Ti(O_2)$, which does not epoxidize alkenes, becomes active in this reaction once it has been transformed to the *cis*-hydroxo(alkyl peroxo) complex, (TPP)Ti(OH)(OOR) [36]. We report here an analysis, using quantum-chemical calculations of the possible evolution of titanium site in the silicalite structure in the presence of water and hydrogen peroxide. The activity of different intermediates in ethylene is considered and the corresponding transition structures of oxygen transfer are also calculated.

A scheme for the possible evolution of a silicalite titanium site is given in Fig. 15. The molecular cluster $Ti(OSiH_3)_4$ has been used to model the initial regular tetrahedral Ti site in silicalite (structure **a** in Fig. 15). The dangling bonds of the Si atoms at the cluster boundaries are saturated with hydrogen atoms. Ab initio calculations have been carried out using LANL1 effective core potentials to describe the inner core electrons of the Ti and Si. Valence electrons were described using the corresponding double zeta quality basis set. The valence double-zeta basis set of

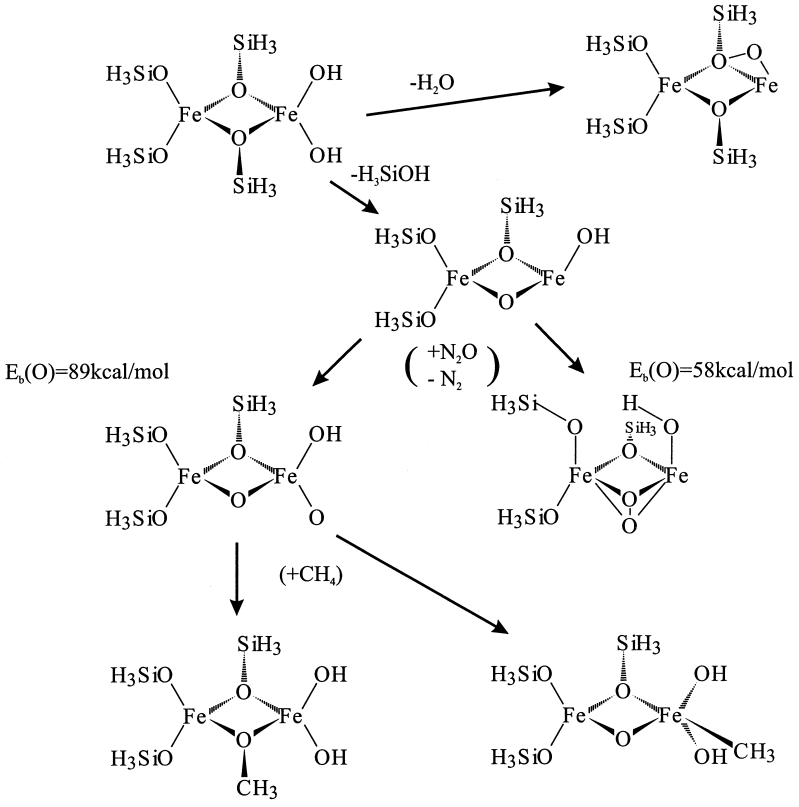

Fig. 14. Cluster models of probable Fe-oxide species in a zeolite cavity and their conversion due to interaction with N_2O and CH_4.

Dunning–Huzinaga has been used for the O and H atoms. The geometry of the clusters was completely optimized at the Hartree–Fock level (HF). Electron correlation was taken into account through single point calculations using the second-order Møller–Plesset perturbation theory (MP2). Fig. 15 shows the structures with titanium peroxo group (**c**) and hydroperoxo group (**d**,**e**) which can be formed in the process of tetrahedral Ti site interaction with the H_2O_2 molecule. The adsorption of H_2O_2, with the formation of a titanium hydroperoxo-complex, is similar to the interaction of the H_2O molecule with titanium silicalite. XANES data [32] on the interaction of H_2O with Ti-silicalite can be interpreted either in terms of the distortion of tetrahedral symmetry or in terms of the incomplete insertion of H_2O in the coordination sphere of Ti (IV). These ideas are in agreement with structures **c** and **d** in Fig. 15. In the case of the peroxo-complex, we have incomplete insertion of ligands in the coordination sphere of the Ti (IV). The Ti–O bond length is equal to 1.78 Å, and the coordinative Ti–O bond length is 2.31 Å. In the case of hydroperoxo–titanium complex, there is a distortion of tetrahedral symmetry; there being two different Ti–O bond lengths of 1.89 and 1.72 Å with O–Ti–O angles of 106.0° and 109.0°. In principle, increasing the coordination number of the hydroperoxo–titanium complex from 4 to 6 is possible due to the interaction of additional ligands with the Ti-containing complex along the C_3 axis [37]. Note, that the optimized Ti–Si distance is significantly longer than in titanium-free zeolites, e.g. 3.1 Å in ZSM-5. Thus, only a flexible mode in the zeolites can permit formation of these structures.

Recently a 5-membered ring was suggested as a possible intermediate in the reaction (structure **e** in Fig. 15) [38]. A 5-membered ring can form through hydrogen bonding of a hydroperoxo-group with a

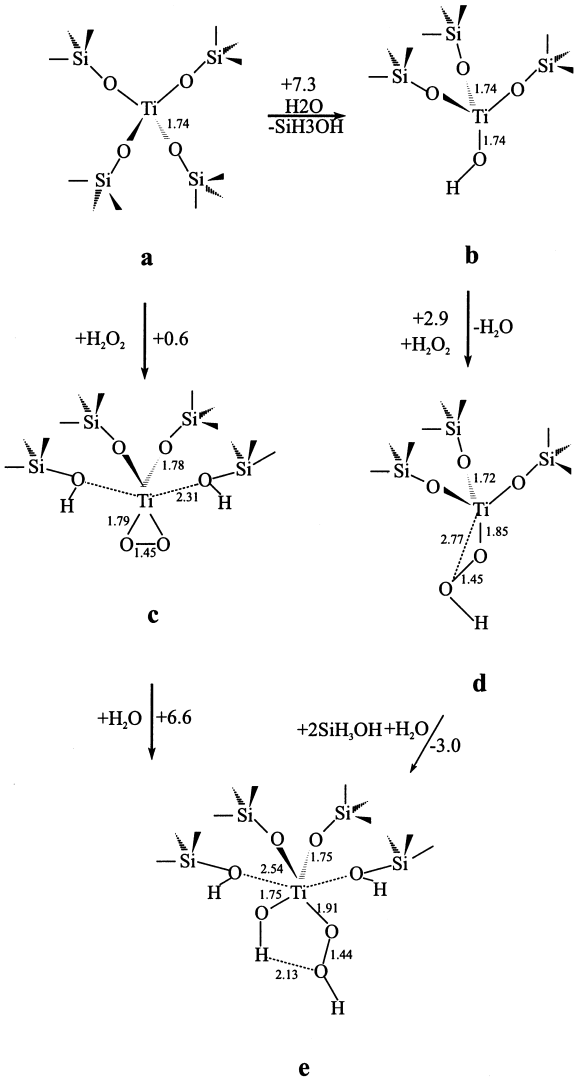

Fig. 15. A scheme for the possible evolution of titanium site, in the presence of water and hydrogen peroxide.

Ti–OH group, solvent molecule or lattice Si–OH group. At this stage of research, it is not possible to establish which species is actually formed in TS-1. Attempts to identify an intermediate *cis*-hydroxo (*t*-Bu-peroxo) complex during the reaction of O=Ti(TPP) with an excess of anhydrous *t*-butyl hydroperoxide, using NMR and UV–Visible spectroscopy failed, perhaps due to its low concentration [36]. The energies of different possible intermediates in the titanium silicalite+H_2O_2/H_2O system have been calculated to analyze the ways in which their transformations and regeneration occur. The results presented in Fig. 15 can be summarized as follows:

1. it is very important to take into account the electron correlation to evaluate the energies of transformations in these systems;
2. the hydroperoxo- and peroxo-complexes of titanium are not energetically unfavourable;
3. all these structures can be in equilibrium if the activation energies for their transformations are small;
4. these structures can participate in the regeneration of the active centers during the epoxidation of ethylene.

The existence of titanyl Ti=O species in silicalite structures has been discussed in the literature. Since we have found that LANL1 potential is not valid to describe the Ti=O bond, the results for the cluster model of this species are given separately in Fig. 16. Both of the structures of Fig. 16 are optimized at the MP2 level, using the 10-electron LANL2 effective core potential to describe the core 1s, 2s and 2p electron shells of the Ti atom. The 3s, 3p and valence shells of Ti have been described by double-zeta quality basis set supplemented to the LANL2 potential. The

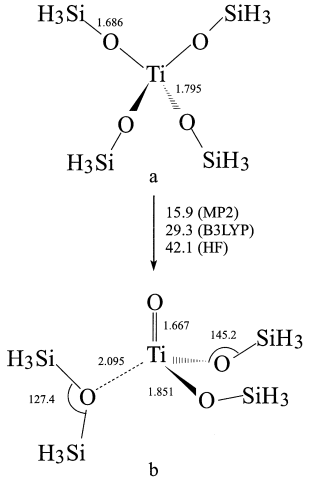

Fig. 16. The structures (Å and degrees) of regular tetrahedral site and Ti=O species models calculated at MP2 level. The energy of transition between the two models is given in kcal/mol. The HF and B3LYP values are calculated with a geometry optimized at the MP2 level.

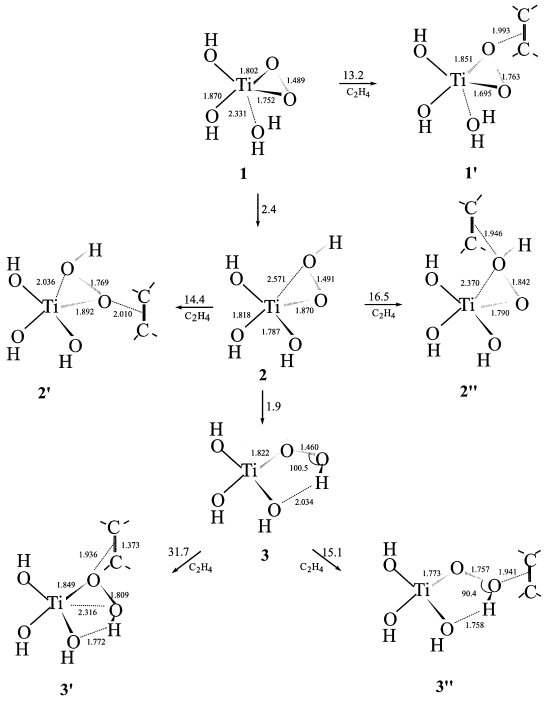

Fig. 17. Models for the intermediates of the reaction (**1**, **2**, **3**) and the corresponding transition states for oxygen transfer to ethylene; geometry in Å and degrees, transition energies in kcal/mol.

6–31 g* and LANL1dz basis sets have been used for the light elements (O,H) and the Si atoms, respectively. The Ti=O bond length of 1.67 Å in a smaller $(HO)_2H_2OTi{=}O$ cluster model calculated within a LANL2 effective core pseudo-potential is in good agreement with the all-electron result for this structure (1.63 Å, Wachters' basis set for Ti), while LANL1 gives a significantly smaller value of 1.50 Å. However, for systems with saturated Ti–O bonds (e.g. for the tetrahedral $Ti(OH)_4$ cluster) the LANL1 potential gives results quite consistent with the all-electrons calculations. The calculated energy of transition from the regular tetrahedral site (Fig. 16(a)) to a structure with a Ti=O group (Fig. 16(b)) shows that the latter is much less stable energetically than the former.

To investigate the activity of different intermediates in ethylene epoxidation, we have calculated at the MP2 level the activation energies of oxygen atom transfer from peroxo- or hydroperoxo-group, to the ethylene molecule. Clusters of minimal size (Fig. 17) have been used for the transition state calculations. The structure of the transition states has been examined at the MP2 level, with the requirement of one negative eigenvalue of a second derivative matrix. The same basis sets as described above (LANL2/DZ and 6-31G*) were used. The calculated geometries and relative energies of the different intermediates (**1**, **2**, **3**) and the corresponding transition structures (**1′**, **2′**, **2″**, **3′**, **3″**) are shown in Fig. 17. All the structures are optimized within the restrictions of a C_s symmetry point group. The most stable is intermediate **1** involving η^2-coordination of the peroxogroup to the Ti atom. However, hydroperoxo species **2** and **3** differ only slightly in energy from structure **1** (2.4 and 4.3 kcal/mol, respectively). The peroxocomplex **1** gives also the lowest energy of the transition state. Transfer of the oxygen atom nearest to the Ti in the hydroperoxo complex **2** (transition state **2′**) takes 2 kcal/mol less than the transfer of a more distant oxygen (**2″**). The transition state **2′** has a η^2-structure with nearly equal distances from the central Ti atom to both oxygens of the hydroperoxogroup. Formation of the 5-membered ring through hydrogen bonding of the hydroperoxo group to one of the Ti–OH moieties leads to a slightly lower barrier for the distant oxygen atom transfer (**3″**) and inhibits the transfer of the oxygen nearest to the Ti of the peroxo group (cf. the barrier of 32 kcal/mol for the transition state **3′**). The latter result can be explained by the difficulty of formation of η^2-structure as in transition state **2′**.

Hence, the results for the minimal models show that the intermediates considered all have comparable values of activation energy for the ethylene epoxidation reaction. However, the activity of transition metal peroxo complexes depends significantly on the coordination number of the metal atom and on the nature of the ligands. Further investigation of larger models is therefore, required to allow final conclusions to be drawn concerning the mechanism of using titanium-silicalites.

Acknowledgements

The authors are grateful to the INTAS programme (project 93-1876), to the Volkswagen Stiftung (project I/68 691) and to the RBRF (projects 96-15-97571 and 97-03-33646) for financial support, as well as to Prof. N. Rösch and Dr. K. Neyman, Technische Universität

München, Munich, Germany for fruitful collaboration during work on the projects.

References

[1] K.I. Zamaraev, G.M. Zhidomirov, Proceedings of the First International Symposium on Relation between Homogeneous and Heterogeneous Catalysis, Novosibirsk, 1986, p. 23.
[2] I.D. Mikheikin, I.A. Abronin, G.M. Zhidomirov, V.B. Kazansky, J. Molec. Catal. 3 (1977) 435.
[3] G.M. Zhidomirov, V.B. Kazansky, Adv. Catal. 34 (1986) 131.
[4] A.G. Pelmenschikov, I.D. Mikheikin, G.M. Zhidomirov, Kinet. Katal. 22 (1981) 1427.
[5] H. Kawakami, S. Yoshida, T. Yonezava, J. Chem. Soc., Faraday Trans. 80 (1984) 205.
[6] E.A. Paukshtis, E.N. Yurchenko, Usp. Khim. 52 (1983) 426.
[7] I.D. Mikheikin, A.I. Lumpov, G.M. Zhidomirov, V.B. Kazansky, Kinet. Katal. 19 (1978) 1053.
[8] A.G. Pelmenschikov, E.A. Paukshtis, V.G. Stepanov, V.I. Pavlov, E.N. Yurchenko, K.G. Ione, G.M. Zhidomirov, J. Phys. Chem. 93 (1989) 6725.
[9] A.G. Pelmenschikov, E.A. Paukshtis, V.G. Stepanov, K.G. Ione, G.M. Zhidomirov, K.I. Zamaraev, Proceedings of the Ninth International Congress on Catalysis, vol. 1, 1988, p. 404.
[10] W.M.H. Sachtler, Z. Zhang, Adv. Catal. 39 (1993) 129.
[11] A.Y. Stakheev, E.S. Shpiro, N.I. Jaeger, G. Schulz-Ekloff, Catal. Lett. 32 (1995) 147.
[12] V.L. Zholobenko, G.-D. Lei, B.T. Carvill, B.A. Lerner, W.M.H. Sachtler, J. Chem. Soc., Faraday Trans. 90 (1994) 233.
[13] A.L. Yakovlev, K.M. Neyman, G.M. Zhidomirov, N. Rösch, J. Phys. Chem. 106 (1996) 3482.
[14] B.I. Dunlap, N. Rösch, Adv. Quantum Chem. 21 (1990) 317.
[15] L.L. Sheu, H. Knözinger, W.M.H. Sachtler, J. Am. Chem. Soc. 111 (1989) 8125.
[16] A.L. Yakovlev, K.M. Neyman, G.M. Zhidomirov, V.A. Nasluzov, N. Rösch, Ber. Bunsenges. Phys. Chem. 106 (1996) 413.
[17] L. Xu, Z. Zhang, W.M.H. Sachtler, J. Chem. Soc., Faraday Trans. 88 (1992) 2291.
[18] R.D. Shannon, K.H. Gardner, R.H. Staley, G. Bergeret, P. Gallezot, A. Auroux, J. Phys. Chem. 89 (1985) 4778.
[19] A.G. Pelmenschikov, I.N. Senchenya, G.M. Zhidomirov, V.B. Kazansky, Kinet. Katal. 24 (1983) 233.
[20] A.G. Pelmenshchikov, R.A. van Santen, J. Jänsen, E. Meijer, J. Phys. Chem. 97 (1993) 11071.
[21] S. Bates, J. Dwyer, J. Phys. Chem. 97 (1993) 5897.
[22] K.M. Neyman, V.A. Nasluzov, G.M. Zhidomirov, Catal. Lett. 40 (1996) 183.
[23] A. Zecchina, E.E. Platero, C.O. Arean, J. Catal. 107 (1987) 244.
[24] M.A. Milov, S.F. Ruzankin, G.M. Zhidomirov, Zhurn. Strukt. Khim., in press.
[25] L.J. Alvarez, L.E. Leon, J.F. Sanz, M.J. Capitan, J.A. Odriczola, J. Phys. Chem. 99 (1995) 17872.
[26] E. Broclawik, H. Himei, M. Yamadaya, M. Rubo, A. Miyamoto, R. Vertrivel, J. Chem Phys. 103 (1995) 2102.
[27] G.I. Panov, V.I. Sobolev, A.S. Kharitonov, J. Mol. Catal. 61 (1990) 85.
[28] M.J. Filatov, A.G. Pelmenschikov, G.M. Zhidomirov, J. Mol. Catal. 80 (1993) 243.
[29] A.V. Arbuznikov, G.M. Zhidomirov, Catal. Lett. 40 (1996) 17.
[30] M.J. Filatov, I.L. Zilberberg, G.M. Zhidomirov, Int. J. Quant. Chem. 44 (1992) 565.
[31] F. Geobaldo, S. Bordiga, A. Zecchina, E. Giamello, G. Leofanti, G. Petrini, Catal. Lett. 16 (1992) 109.
[32] S. Bordiga, S. Coluccia, C. Lamberti, L. Marchese, A. Zecchina, F. Boscherini, F. Buffa, F. Genoni, G. Leofanti, G. Petrini, G. Vlaic, J. Phys. Chem. 98 (1994) 4125.
[33] G. Bellussi, M.S. Rigutto, Rigutto advanced zeolite science and applications, Stud. Surf. Sci. Catal. 95 (1994) 177.
[34] M.G. Clerici, P. Ingallina, J. Catal. 140 (1993) 71.
[35] R.A. Sheldon, J. Mol. Catal. 7 (1980) 107.
[36] H.J. Ledon, F. Varescon, Inorg. Chem. 23 (1984) 2735.
[37] P.E. Sinclair, G. Sankar, C.R.A. Catlow, J.M. Thomas, T. Maschmeyer, J. Phys. Chem. 101 (1997) 4232.
[38] W. Adam, A. Corma, A. Martinez, C.M. Mitchell, T.I. Reddy, M. Renz, A.K. Smerz, J. Mol. Catal. A 117 (1997) 357.